JPRS L/9917

18 August 1981

USSR Report

EARTH SCIENCES

(FOUO 6/81)

FBIS FOREIGN BROADCAST INFORMATION SERVICE

NOTE

JPRS publications contain information primarily from foreign newspapers, periodicals and books, but also from news agency transmissions and broadcasts. Materials from foreign-language sources are translated; those from English-language sources are transcribed or reprinted, with the original phrasing and other characteristics retained.

Headlines, editorial reports, and material enclosed in brackets [] are supplied by JPRS. Processing indicators such as [Text] or [Excerpt] in the first line of each item, or following the last line of a brief, indicate how the original information was processed. Where no processing indicator is given, the information was summarized or extracted.

Unfamiliar names rendered phonetically or transliterated are enclosed in parentheses. Words or names preceded by a question mark and enclosed in parentheses were not clear in the original but have been supplied as appropriate in context. Other unattributed parenthetical notes within the body of an item originate with the source. Times within items are as given by source.

The contents of this publication in no way represent the policies, views or attitudes of the U.S. Government.

APPROVED FOR RELEASE: 2007/02/09: CIA-RDP82-00850R000400040029-2

JPRS L/9917

18 August 1981

USSR REPORT

EARTH SCIENCES

(FOUO 6/81)

CONTENTS

APPROVED FOR RELEASE: 2007/02/09: CIA-RDP82-00850R000400040029-2

OCEANOGRAPHY

YASTREBOV OUTLINES PROGRESS IN UNDERWATER RESEARCH

Moscow SOVIET UNION in English No 5 (374), May 81 pp 16-19

[Interview with Prof Vyacheslav Yastrebov, doctor of technical sciences, deputy director of the Institute of Oceanology, USSR Academy of Sciences, by SOVIET UNION correspondent A. Chuba; date and place not specified: "The Ocean: 56 Steps Into the Deep"]

[Text] The testing of the "Oceanolog", a new manned underwater vessel, was completed in the autumn of 1980 near Novorossiisk. It moved about easily in the water, manoeuvred and handled well, and, when necessary, could hover over a given point. Its arm--an electro-hydraulic trailing manipulator--confidently held a geologist's hammer, scoop, ground pipe for taking samples, and other instruments. During one of their descents the hydronauts --Commander Vladimir Gromov, mechanic Nikolai Tokovenko and observer Yuri Belyayev--reached a depth of 609 metres, a record for this type of apparatus. The "Oceanolog", developed by designers from the USSR Ministry of the Fishing Industry in fulfillment of an order of the Far Eastern Scientific Centre of the USSR Academy of Sciences, became the 56th device built in this country for underwater experiments and projects.

Soviet Union correspondent A. Chuba interviewed Professor Vyacheslav Yastrebov, D.Sc. (Techn.), deputy director of the Institute of Oceanology of the USSR Academy of Sciences, who discusses the tasks facing researchers of the ocean depths, and how modern technology is making it possible to tackle them.

The exploration of the ocean depths is often compared to the conquest of outer space. There is a measure of logic to this comparison, as the world ocean, like the expanse of outer space, has an enormous influence on many earthly processes, and it is just as difficult for man to penetrate it; as is the case with outer space, he has to create special apparatuses with reliable life-support systems. Regrettably, we know the ocean's depths, which man has been trying to penetrate since time immemorial, only slightly better than outer space, exploration of which was launched a quarter of a century ago. Meanwhile, man has no less a vital interest in the ocean than in the extraterrestrial expanses. The exploration of the

world ocean is directly connected with the solution of such crucial issues facing the planet today as the food, energy and raw materials problems.

From the standpoint of science, priority in researching the ocean depths should be relegated to the prominent oceanologist Jacques-Yves Cousteau, the inventor of the aqualung and the famous Diving Saucer research minisubmarine. From 1962 to 1965 he headed the Precontinent Programme, which launched underwater research projects according to plan. Groups of aquanauts who lived on the ocean floor in special houses (the idea of the diving bell, known since the times of Alexander of Macedon, was used in their construction), conducted systematic observations of the inhabitants of the sea, collected geological specimens and carried out trial assembly and exploitation of equipment for sea oil rigs.

In the Soviet Union, a large part of whose borders lies on seas and oceans and which therefore has a vital stake in their exploration, such research began approximately at that time, in 1966, with the Ikhtiandr programme. For three years in a row various types of underwater abodes were tested along the Crimean shores, and medical experiments made. Later other Soviet programmes, including the Chernomor programme, prepared by scientists from our institute, were implemented as well. It had a purely oceanological thrust. The research project, in which oceanologists, marine biologists, geologists, hydrophysicists and hydro-opticians took part, showed the high level of the efficiency of the underwater structures for conducting a wide range of operations and experiments.

To be used for these purposes now is a diving complex which is installed on the "Vityaz" research vessel, the successor of the famous "Vityaz", aboard which Soviet scientists discovered life at a depth of some ten kilometres and pinpointed the deepest spot in the Mariana Trench near the Island of Guam (11,022 metres), and carried out other important research projects. The new "Vityaz" will make its first trip this year.

A special arm of underwater technology is equipment which is capable of moving about underwater, descending to the bottom and doing various types of work there. The underwater apparatus enables the scientist to be an eyewitness to processes occurring in the deep, to the life of its denizens, and to collect specimens and take photographs. Many interesting structures have been built in this country and abroad over the past 20 years. These are the American underwater research ship, the "Ben Franklin", which completed a drift in the depths of the Gulfstream, the French bathyscaph "Archimede", the Japanese "Shinkai" and many others. Several of them, such as the "Trieste", which reached the bottom of the Mariana Trench, were "preprogrammed" to conquer record depths and can function solely as a kind of lift. Meanwhile the range of tasks the underwater devices have to handle is growing from one year to the next. They are now servicing ocean oil rigs, prospecting minerals and fish resources, doing rescue and repair work, and carrying out a series of oceanological research projects. It is only natural that like "land" equipment, they should have their own trucks and passenger vehicles, mobile laboratories and all-purpose vehicles, and other specialised means.

A whole series of manned underwater apparatuses has been developed and is being used in the Soviet Union. These are the "Sever-2", "Shelf-1", "Tetis", "Argus", "Tinro-2", "Bentos-300", "Atlant-1" and "Atlant-2", "Oceanolog" and others.

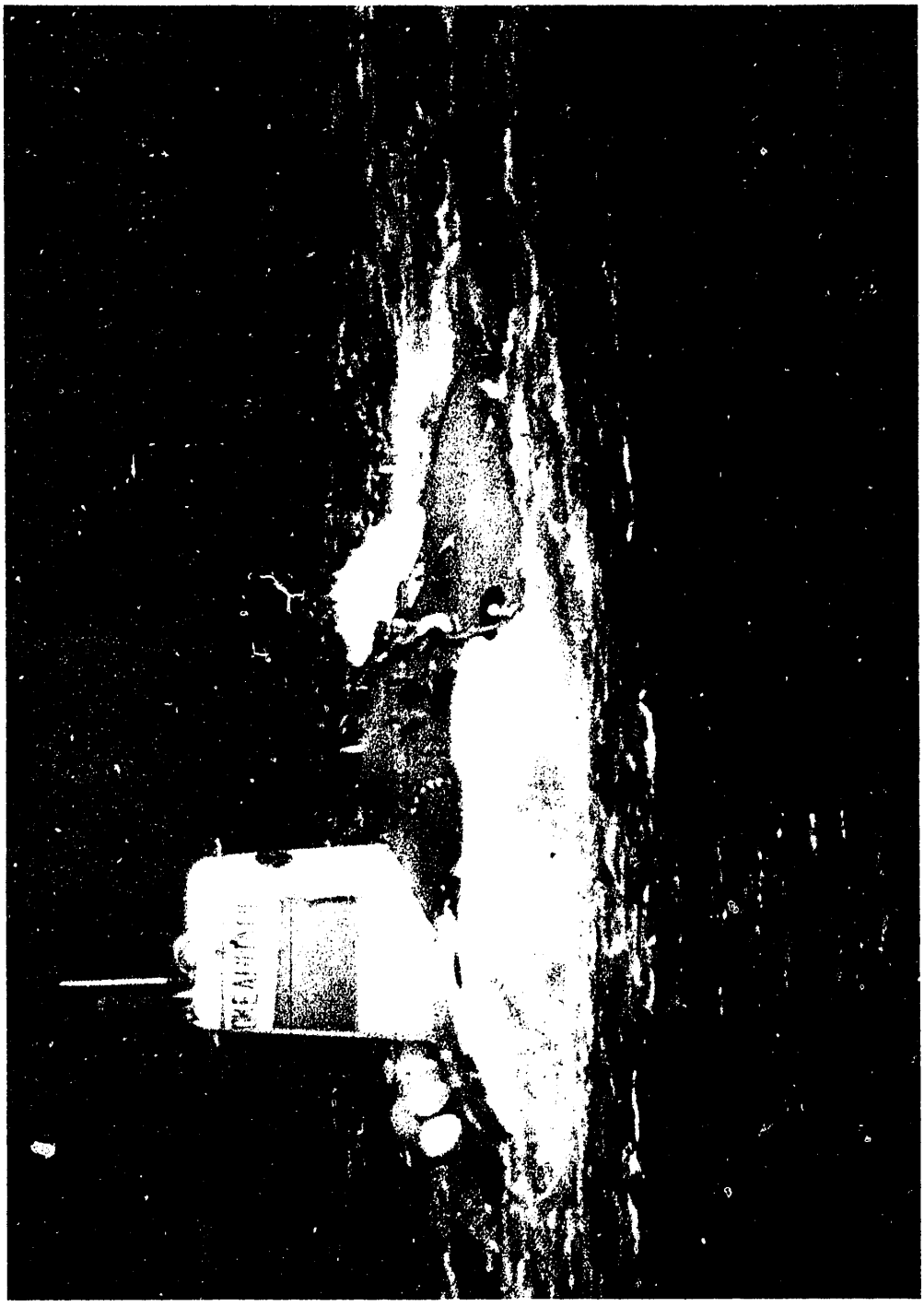

The "Oceanolog is one of the latest vessels built in the USSR for underwater research.

The "Tinro-2" underwater research boat, designed for scientific work and observation of schools of fish and of commercial fishing nets.

Once every two years countrywide seminars for designers of underwater equipment for research are held in Gelendzhik, on the Black Sea. Above: the "Argus" manned underwater apparatus, and the "Skat" second-generation aqua-robot. Below: the "Manta-1.5" remote-controlled manipulator.

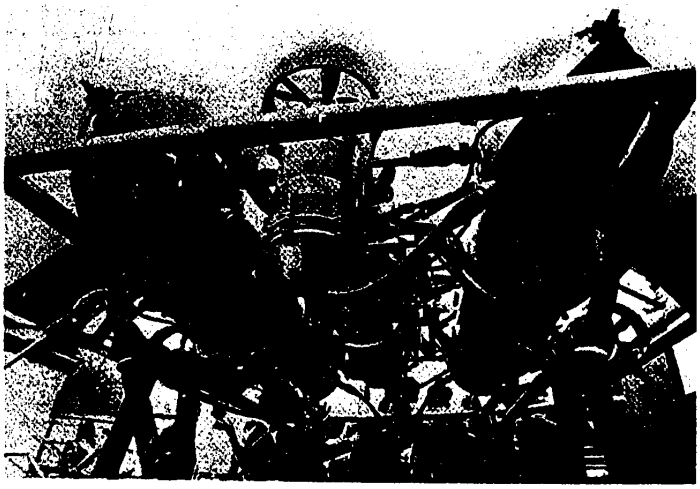

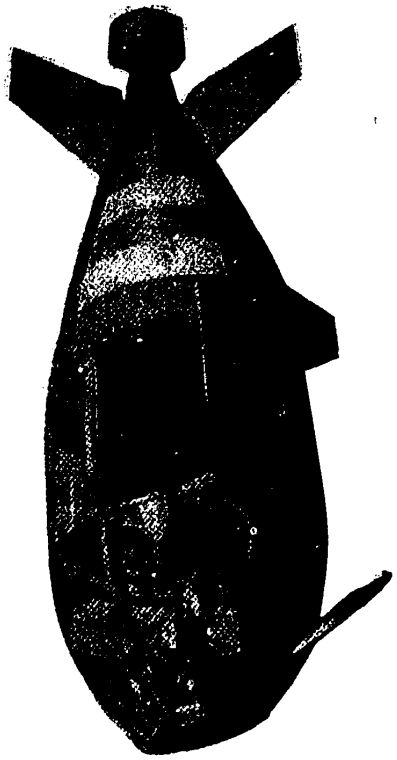

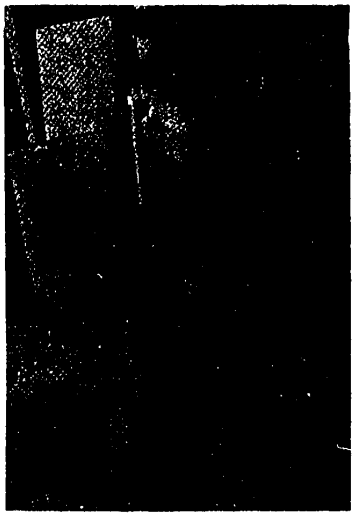

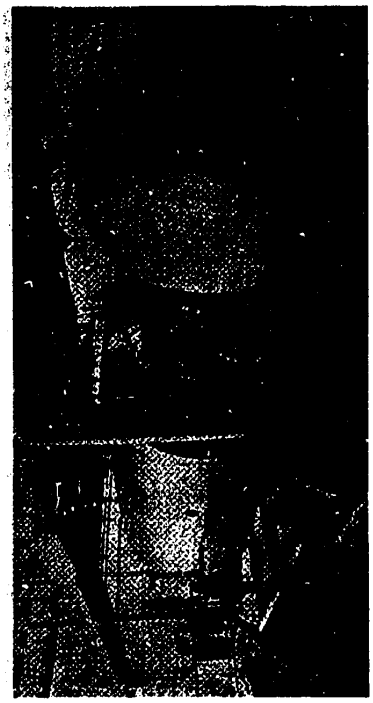

Above: the "Zvuk-4m" remote-controlled apparatus for photographing at great depths; and an underwater "limousine" for divers.

Below: a pressure complex for training specialists to do research in conditions of increased pressure in their underwater abode.

All of them are different in terms of size, depth of descent and self-sufficiency. Some, for instance, are designed for planting underwater "orchards" of seaweed; others help fishermen; still others are adapted for taking precise measurements and doing scientific work.

The "Bentos-300", for example, is one of the world's largest underwater research vessels, with a 14-man capacity. It has a displacement of up to 500 tons, and can operate underwater independently for 14 days. It is equipped with a device for ejecting a diver deep below the surface. The "Bentos" makes it possible to do extensive research for the fishing industry, and it is used in various fields of scientific research as well.

The deep-underwater apparatus "Sever-2" possesses great possibilities. Five researchers can descend to a depth of 2,000 m and, taking advantage of the great manoeuvrability of the vessel, observe the movement of schools of fish and the operation of fish nets, and conduct various tests. The apparatus is equipped with five independent emergency ascent systems, and an effective fire-fighting system.

The actual presence of a scientist in the underwater world has done a great deal to change and enrich our conception of the life of the ocean. It has turned out, for example, that trawlers catch far from all the types of fish inhabiting the deep, and the devices lowered from a vessel to take samples of the bottom give an incomplete picture of the composition of the ocean floor. Underwater apparatuses have enabled scientists to conduct research impossible with other methods, and to obtain new information about the structure of the earth's crust, the movement of mainlands and the earth's geological and historical past. Small apparatuses, such as the "Argus", designed at our institute, are usually used for doing such research. The "Argus" is six metres long and has a displacement of 8.5 tons. The three-man crew can descend to a depth of 600 m and work underwater for eight hours.

There are situations, however, when using a manned vessel is either impossible or irrational. In such instances its functions are assumed by an automatic device, a kind of oceanic robot. The underwater robots have invariably been a part of Soviet oceanological expeditions in recent years. Our institute's remote controlled apparatuses the "Crab", "Manta-1.5", "Zvuk-4m", "Zvuk-6" and others can operate at great depths. The underwater devices successfully showed what they can do during last year's expedition, which analysed zones of fractures in the earth's crust (rift zones) in the Red Sea. They enabled scientists to put together a unique collection of samples of Red Sea basalts, take more than 4,000 photographs and shoot a long-length video film. The scientists discovered stones on the bottom on which there is practically no sediment, "pipes" of fresh volcanic lava, and mountains split from foot to peak. This means that today, too, movements of the earth's crust continue, and processes are taking place which are shaping the face of the planet.

Our institute has at its disposal all types of underwater vessels: manned, towed, remote controlled with manipulators, robots. We are soon to add the "Skat"--a second-generation aqua-robot. For the time being there is no information about the existence of such robots in other countries. Unlike the remote-controlled apparatuses, there is no cable between the mothership and the "Skat". All the robot's actions, depending on the floor's relief and the outside situation, are

guided by a built-in computer. The "Skat" has a "memory"; it can acquire elementary skills, independently adapt to the atmosphere on the bottom and take photographs.

The "Skat" is the latest rung in the ladder of man's exploration of the ocean depths. He has made a start, but there is still a long way to go.

CSO: 1852/5

UDC 551.466.2

INFLUENCE OF INTERNAL GRAVITATIONAL WAVES ON THE SPECTRUM OF WIND WAVES

Sevastopol' MORSKIYE GIDROFIZICHESKIYE ISSLEDOVANIYA in Russian No 1(88), Jan-Mar 80 (manuscript received 17 Mar 80) pp 44-55

[Article by Yu. M. Kuftarkov and V. N. Kudryavtsev]

[Text]

Abstract: The transformation of the spectrum of wind waves under the influence of a variable current induced by an internal wave is examined. The spectral density of the wave effect is described by a kinetic equation whose right-hand side includes a Miles generation source with nonlinear limitation of amplitude. Under definite conditions it is possible to obtain an analytical solution in the phase plane region corresponding to trapped waves. The transformation of the Phillips spectrum under the influence of an internal gravitational wave is illustrated.

Interest in study of evolution of the spectrum under the influence of a current induced by an internal wave is associated both with the problem of sensing of internal waves by remote methods and the need for a detailed investigation of the mechanisms of generation of wind waves. At the present time there is no finalized theory which could predict the evolution of the spectrum of wind waves in the field of internal gravitational waves. Theoretical investigations in this direction have been limited to one degree or another. For example, in [1] in an adiabatic approximation a study was made of the effect of modulation of the parameters of surface waves on a current induced by a long wave. In this study it was shown that the most significant changes in the parameters of the wave packet occur in a case when its group velocity c_g is close to the phase velocity c of the internal wave. The concept of blocking points, in which $c_g = c - U$ (U is the velocity induced by the internal wave) is introduced. These points are kinematically limited, beyond which propagation of the wave packet is impossible. It was postulated that at these points the packet is present for an unlimited length of time, so that the energy increases exponentially without limitation due to the work of radiation stresses. In later studies [4, 5] it was shown that the blocking points are the points of reflection of wave packets and therefore the singularity associated with an unlimited increase in energy is excluded. A detailed analysis of evolution of the parameters of an adiabatic wave packet with allowance for reflection and capture by an internal wave was given in [3]. A more realistic situation is examined in [7],

where a wave generation source (Miles generation mechanism) was added to the spectral equation. However, no consideration is given to wind waves with a group velocity close to the phase velocity of the internal wave.

This study is devoted to an investigation of the reaction which can be noted in a wind wave spectrum in the gravitational interval to internal waves. In contrast to the mentioned studies, there are no limitations on the region of wave numbers of surface waves, on the one hand, and on the other hand energy gains and losses have been included in the spectral equation.

Equations of Model

The evolution of the spatial spectrum of the wind effect ψ on a variable current caused by internal waves is described by the equation

$$\frac{\partial \psi}{\partial t} + \frac{\partial \Omega}{\partial k_\beta}\frac{\partial \psi}{\partial x_\beta} - \frac{\partial \Omega}{\partial x_\beta}\frac{\partial \psi}{\partial k_\beta} = \frac{Q}{\omega}, \qquad (1)$$

where $\psi = \varphi/\omega$; φ is the spectral density of energy; ω is frequency in the reckoning system in which the medium is locally at rest; $\Omega(\vec{k}, \vec{x}, t)$ is the known dispersion relationship; Q is a function modeling concentrated effects for a particular spectral component.

The explicit form of Q is determined in each specific case in dependence on the degree of interaction of the wind wave components with one another and with different movements both in the ocean and in the near-water layer of the atmosphere.

In accordance with [7], we will represent the source Q in the form

$$\frac{Q}{\omega} = \alpha\psi - \alpha\frac{\psi^2}{\psi_0}, \qquad (2)$$

where α is the wind-wave interaction coefficient. The second term in (2) is a nonlinear limitation of the exponential energy increase and determines the existence of some stationary spectrum $\psi_c(k)$.

For a full description of wind waves in a nonuniform current induced by internal waves it is necessary that a kinematic relationship for the wave vectors be added to equation (1)

$$\frac{\partial k_\gamma}{\partial t} + \frac{\partial \Omega}{\partial k_\beta}\frac{\partial k_\gamma}{\partial x_\beta} = -\frac{\partial \Omega}{\partial x_\gamma}, \quad \frac{\partial k_\gamma}{\partial x_\beta} = \frac{\partial k_\beta}{\partial x_\gamma}. \qquad (3)$$

Then U = U(x - ct) and as a simplification we examine a one-dimensional case: the x-axis is directed along the propagation of surface waves and the internal waves can be both codirectional (phase velocity $c > 0$) and oppositely directed to the surface waves ($c < 0$). The case of codirectionality is most complex for analysis in connection with the phenomenon of capture of surface waves by internal waves. The opposite variant causes no analytical difficulties and will be examined below for a possibly greater completeness of the model.

Instead of equations in partial derivatives (1), (3) we will write an equivalent characteristic system of ordinary differential equations [expression (6) is given in a coordinate system moving with the phase velocity of an internal wave]

$$\frac{\partial \psi}{\partial t} = \alpha\psi - \alpha\frac{\psi^2}{\psi_0}, \tag{4}$$

$$\frac{\partial k}{\partial t} = -\frac{\partial \Omega}{\partial x}, \quad \frac{\partial x}{\partial t} = \frac{\partial \Omega}{\partial k}, \tag{5}$$

$$\Omega = (gk)^{1/2} + k(U - C). \tag{6}$$

In completing formulation of the problem we will write the initial conditions

$$\psi = \psi_0(k_0), \quad k = k_0, \quad x = x_0. \tag{7}$$

Leaving to one side for the moment the problems associated with the kinematics of the wave packets, we will write a solution for the spectral density of the wave effect

$$\frac{1}{\psi(k,x,t)} = \frac{1}{\psi_0(k)} - \int_0^t \frac{d}{dk}\left(\frac{1}{\psi_0(k)}\right)\frac{dk}{dt} \exp\left[-\int_{t_1}^{t} \alpha(k)\,dt_2\right] dt_1. \tag{8}$$

With (5) and (6) taken into account, the latter formula assumes the form

$$\frac{1}{\psi(k,x,t)} = \frac{1}{\psi_0(k)} + \int_0^t k\frac{\partial U}{\partial x}\frac{d}{dk}\left(\frac{1}{\psi_0(k)}\right) \exp\left[-\int_{t_1}^{t} \alpha(k)\,dt_2\right] dt_1. \tag{9}$$

This solution was represented in [7], but, as was noted above, it was analyzed only for the region of wave numbers satisfying the condition

$$\left|\frac{c_g(k) - C}{C}\right| \sim 1.$$

Kinematics of Wave Packets

The problem of the motion of a wave packet in phase space includes both a determination of the trajectory of motion and the position of the packet on the trajectory at each moment in time. Along the characteristics (5) $d\Omega/dt = \partial\Omega/\partial t \equiv 0$ and accordingly the equation

$$\Omega = (gk)^{1/2} + k\left[U(x) - C\right] = const \tag{10}$$

determines the type of trajectory in phase space.

We will examine a case when the velocity U induced by the internal wave has the form

$$U = U_m \cos k_i x. \tag{11}$$

Using formula (11), using expression (10) it is easy to construct the trajectory of wave packets for the case $c > 0$ in the phase plane (k, x) (Fig. 1). The closed curves correspond to trapped waves and the unclosed curves correspond to untrapped waves. The phase plane region situated above the dashed line corresponds to "retrograde" waves ($\partial\Omega/\partial k < 0$), that is, wave packets which in the considered coordinate system move in the negative direction of the x-axis. The region situated below the dashed line corresponds to direct waves ($\partial\Omega/\partial k > 0$) which are propagated in a positive

direction. The intersections of the dashed line, determined by the equation

$$\frac{1}{2}\left(\frac{g}{k}\right)^{1/2} - c + U_m \cos k_i x = 0,$$

with the trajectories of the wave packets are the "turning points," that is, the points of merging of the straight lines and the "return" branches of equation (10).

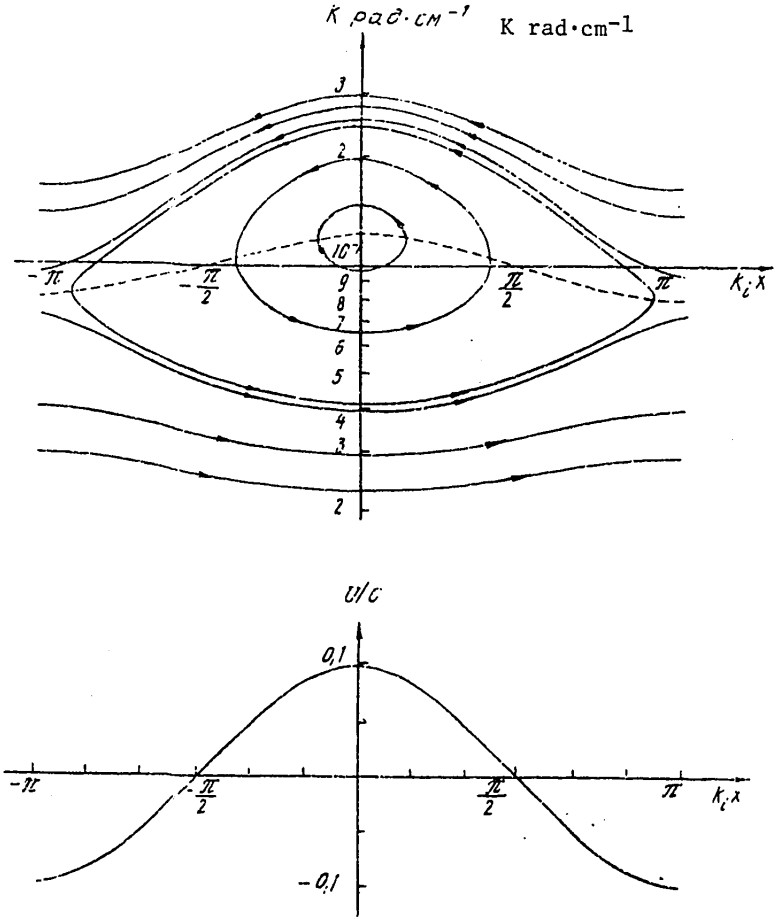

Fig. 1.

A detailed analysis of the linearized dispersion relationship for trapped waves was given earlier in [3]. However, the linearization carried out for the U_m/c parameter in the last analysis led to great restrictions of the U_m/c value ($U_m/c < 10^{-2}$). Internal ocean waves are characterized by $U_m/c \sim 10^{-1}$. Accordingly, in a general case in the analysis of the kinematics of wave packets in the velocity

field induced by an internal wave it is necessary to use a nonlinear dispersion relationship.

We will determine the position of the wave packets on the trajectory in time. In a general case it is impossible to make an analytical determination of k(t) and x(t) from system (5), (6). However, some asymptotic solutions meriting special attention can be found.

We will examine the region of the phase plane corresponding to the condition [in a case when surface and internal waves have opposite directions the entire phase plane satisfies this condition]

$$\left|\frac{\frac{1}{2}\left(\frac{g}{k}\right)^{1/2}-C}{C}\right| \sim 1 .$$

Using an ordinary asymptotic scheme, we represent k and x in the form

$$k(t)=k_0+\tilde{k}(t), \quad x(t)=\hat{x}(t)+\tilde{x}(t), \tag{12}$$

where $\hat{x}(t) = x_0 + [c_g(k_0) - c]\,t$. It is easy to demonstrate that the disturbances $\tilde{k}$ and $\tilde{x}$ have the order of magnitude $O(U/c_g - c)$, and equations (5), (6) can be written in the form

$$\begin{aligned}\frac{d\tilde{k}}{dt}&=-k_0\left(\frac{\partial U}{\partial x}\right)\Big|_{x=\hat{x}}+O\left[\left(\frac{U}{c_g-C}\right)^2\right],\\ \frac{d\tilde{x}}{dt}&=-\frac{1}{2}c_g(k_0)\frac{\tilde{k}}{k_0}+U\Big|_{x=\hat{x}}+O\left[\left(\frac{U}{c_g-C}\right)^2\right].\end{aligned} \tag{13}$$

Substituting the solution of this system into the expansions (12), we obtain

$$k(t)=k_0\left\{1-\frac{U_m}{c_g(k_0)-C}\left[\cos k_i\hat{x}-\cos k_i x_0\right]\right\}, \tag{14}$$

$$\begin{aligned}x(t)=\hat{x}+\frac{U_m}{k_i\left[c_g(k_0)-C\right]}\left(\sin k_i\hat{x}-\sin k_i x_0\right)\cdot\\ \cdot\left[1+\frac{1}{2}\frac{c_g(k_0)}{c_g(k_0)-C}\right]-\frac{t}{2}\frac{c_g(k_0)\,U_m}{c_g(k_0)-C}\cos k_i x_0 .\end{aligned} \tag{15}$$

Formulas (14), (15) give the position of the wave packet on the phase plane in time. Expressions (14), (15) were cited earlier (but with a different order of accuracy) in [7]. With $c_g \ll c$ (slow ripples on a fast long wave) from (14) we have the degree of variability of the wave number, which is equal to U/c. This in actuality corresponds to the result obtained in [8].

In another limiting case ($c_g \gg c$), which corresponds to fast surface waves on a slow, long internal wave, the degree of variability of the wave number, as can be seen from (14), is equal to U/c_g [6].

It was not possible to obtain an analytical solution in the region of the phase plane corresponding to trapped waves. However, as will be demonstrated below, this circumstance in a number of cases is not fundamental in an investigation of evolution of the spectrum of surface waves interacting with the wind.

Evolution of Wave Packet Spectral Density

The spectral density of the energy of wave packets in the region of untrapped waves ($|c_g - c/c| \sim 1$) is determined from expression (9) with the use of formulas (14), (15). For a specific field $U = U_m \cos k_i x$ the expression for spectral density (with $\alpha t \to \infty$) is given in [7] and has the form

$$\psi(k,x) = \psi_0(k) + \frac{\omega_i U_m}{\alpha(k_0) C} k_0 \frac{d\psi_0(k_0)}{dk}\Big|_{k=k_0} \frac{\cos(k_i x + \theta)}{\sqrt{1+\left(\frac{\omega_i}{\alpha(k_0)}\right)^2\left(\frac{c_g(k_0)}{C}-1\right)^2}} + O\left[\left(\frac{U}{C}\right)^2\right], \qquad (16)$$

where

$$\theta = \operatorname{arctg} \frac{\alpha(k_0)/\omega_i}{c_g(k_0)/C - 1}$$

is a value determining the phase shift associated with interaction of the wave packet and the wind; ω_i is the frequency of the internal wave. In expression (16) the variables k and x are functions of time and determine the position of the packet on its trajectory. We note that in the case of an opposite direction of surface and internal waves the solution (16) is correct for any k.

We will ascertain the spectral density ψ of wave packets trapped by the internal wave. For nonblocking wave packets the wave number disturbances are small

$$\left[O\left(\frac{U}{c_g - c}\right)\right].$$

This was taken into account in the derivation of expressions (13), (16). For trapped waves (Fig. 1) the wave number of the packet can change its order of magnitude. Accordingly, the asymptotic scheme of the expansion (12) is not applicable for the evolution of the spectral density of trapped waves. However, this difficulty can be overcome if use is made of physical considerations associated with the relationship between the rates of change in the energy of the wave packet during its interaction with the wind and an internal wave.

An analysis of the integrand in (9) gives basis for assuming that in a number of cases the adiabatic function

$$\Phi(k_i, x) = k \frac{\partial U}{\partial x} \frac{d}{dk}\left(\frac{1}{\psi_0(k)}\right)$$

is slow relative to the fast exponent. In other words, the adiabatic changes in spectral density for the region of trapped waves are slow in comparison with the characteristic time of surface wave generation.

Assume that T and α^{-1} are the characteristic times of adiabatic and wind variability of the packet respectively. Then the preceding assertion is correct with satisfaction of the condition $\alpha^{-1}/T \ll 1$.

For an evaluation of the coefficient of interaction of the wind with surface waves we will use the empirical approximation

$$\alpha/\omega \sim 10^{-2}\frac{U_*}{(g/k)^{1/2}} \quad [7].$$

We will determine the evaluation α^{-1} and the understated evaluation T:

$$\alpha/\omega \sim 10^{-2}\frac{U_*}{2C}, \quad T \sim \omega_i^{-1}.$$

Then with $\omega_i \ll 10^{-4}\cdot gW/c^2$ the ratio $\alpha^{-1}/T \ll 1$. In the latter expressions W is the wind velocity related to dynamic velocity U_* in the following way: $U_*^2 \sim 10^{-3}W^2$. For the phase velocity value $c^2 \sim 10^3 cm^2\cdot sec^{-2}$, characteristic for internal ocean waves and wind $W \sim 5\cdot 10^2$ cm·sec^{-1}, the upper value of the frequency is $\omega_i^{up} \sim 5\cdot 10^2$ rad·sec^{-1}.

Thus, for the frequencies of internal waves satisfying $\omega_i \ll \omega_i^{up}$ the integrand adiabatic function Φ in (9) is "slow" relative to the "fast" exponent. This makes it possible to expand $\Phi(k, x)$ and

$$\int_{t_1}^{t}\alpha(k)\,dt_2$$

into a Taylor series in the neighborhood of the time t determining the position of the packet on the phase plane

$$\Phi(t_1) = \Phi(t) + \frac{d\Phi(t_1)}{dt_1}\Big|_{t_1=t}(t_1 - t) + O\left[\left(\frac{\omega_i}{\alpha}\right)^2\right], \qquad (17)$$

$$\int_{t_1}^{t}\alpha(k)\,dt_2 = -\alpha\left[k(t)\right](t_1 - t) + O\left[\frac{\omega_i}{\alpha}\,\frac{U}{C}\right],$$

where

$$\frac{d\Phi}{dt} = \frac{\partial U}{\partial x}\frac{d}{dk}\left(\frac{1}{\psi_0}\right)\frac{dk}{dt} + k\frac{\partial^2 U}{\partial x^2}\frac{d}{dk}\left(\frac{1}{\psi_0}\right)\frac{dx}{dt} + k\frac{\partial U}{\partial x}\frac{d}{dk^2}\left(\frac{1}{\psi_0}\right)\frac{dk}{dt}. \qquad (18)$$

Substituting formulas (17) into expression (9), we obtain, after integration and proceeding to the limit with $\alpha t \to \infty$

$$\frac{1}{\psi} = \frac{1}{\psi_0} + \frac{\Phi}{\alpha}\left[1 - \frac{1}{\alpha\Phi}\frac{d\Phi}{dt}\right] + O\left[\left(\frac{\omega_i}{\alpha}\right)^3\cdot\frac{U}{C}\right].$$

The latter formula, with the use of (18), can be written

$$\psi = \psi_0 - \frac{\psi_0^2}{\alpha}\frac{\partial U}{\partial x}k\frac{d}{dk}\left(\frac{1}{\psi_0}\right)\left[1 - \frac{C}{\alpha}\left(\frac{c_g}{C} - 1\right)\frac{\partial^2 U}{\partial x^2}\Big/\frac{\partial U}{\partial x}\right] + O\left[\max\left(\frac{\omega_i}{\alpha}\right)^3\frac{U_m}{C}, \left(\frac{\omega_i}{\alpha}\,\frac{U}{C}\right)^2\right], \qquad (19)$$

For a specific velocity field stipulated by expression (11) for the spectral density of the wave effect we obtain the expression

$$\psi=\psi_0+\frac{\omega_i}{\alpha}\frac{U_m}{C}\sqrt{1+\left[\frac{\omega_i}{\alpha}\left(\frac{c_g}{C}-1\right)\right]^2}\,k\frac{d\psi_0}{dk}\left[\cos\left(k_i x+\theta\right)\right]. \qquad (20)$$

This solution is correct for trapped wave packets in a case when $\omega_i/\alpha \ll 1$. Comparing (20) with the solution obtained for the region of the phase plane of untrapped waves, it is easy to see that with $\omega_i/\alpha \ll 1$ with an accuracy to

$$O\left[\left(\frac{\omega_i}{\alpha}\right)^3\frac{U}{c}\right]$$

it coincides in form with the solution (16). Accordingly, solution (16) is uniformly suitable in the entire phase plane, including the region of trapped waves, if in (16) all the functions on the right-hand side are considered functions of the moving coordinates of the wave packet.

Transformation of Phillips Spectrum

The theoretical model proposed above is applicable for describing the dynamics of one wave packet. But since in a real situation the wave field is represented by a superposing of a great number of wave packets, formula (16) can be regarded as an expression for the spectrum of surface waves in any phase of the internal wave determined by the coordinate x.

We will investigate the variability of wind waves approximated by the Phillips spectrum

$$\varphi(k)=\begin{cases}Bk^{-3} & \text{when } k\geqslant k^*,\\ 0 & \text{when } k<k^*,\end{cases} \qquad (21)$$

where B is a constant; k^* is the wave number of the spectral peak, which is determined from the empirical relationship $(g/k^*)^{1/2}=W$. For this we substitute (21) into expression (16). As a result, for the relative change in the spectral density of energy $\varphi=\omega\psi$ we obtain the expression

$$\varphi(k,x)=Bk^{-3}\left[1-\frac{1}{2}\frac{U_m}{C}\frac{\omega_i}{\alpha(k)}\frac{\cos\left(k_i x+\theta\right)}{\sqrt{1+\left[\frac{\omega_i}{\alpha}\left(\frac{c_g}{C}-1\right)\right]^2}}\right]. \qquad (22)$$

As was demonstrated above, this solution is equally suitable in the region of trapped waves under the condition $\omega_i/\alpha \ll 1$.

Figure 2 shows the normalized spectral density of energy for different phases of an internal wave propagating in the direction of the x-axis ($c>0$), computed using formula (22). The curves were plotted for the following values of the parameters: $U_m/c = 10^{-1}$, $c = 60$ cm·sec^{-1}, $k^* = 3\cdot10^{-1}$ rad·cm^{-1} ($W = 6$ m·sec^{-1}), $\omega_i = 3\cdot10^{-3}$ rad·sec^{-1}. In the computations use was made of an empirical expression for the coefficient of wind-wave interaction [7]

$$\alpha=10^{-2}kU_*\cos\theta'\left(1+1{,}6\left|\cos\theta'\right|U_*/c\right)\left\{1-\exp\left[-8{,}9\left(U_*/c-0{,}03\right)^{1/2}\right]\right\}$$

Here c is the phase velocity of the spectral component of surface waves; θ' is the angle between the vectors $\vec{c}$ and $\vec{U}_*$.

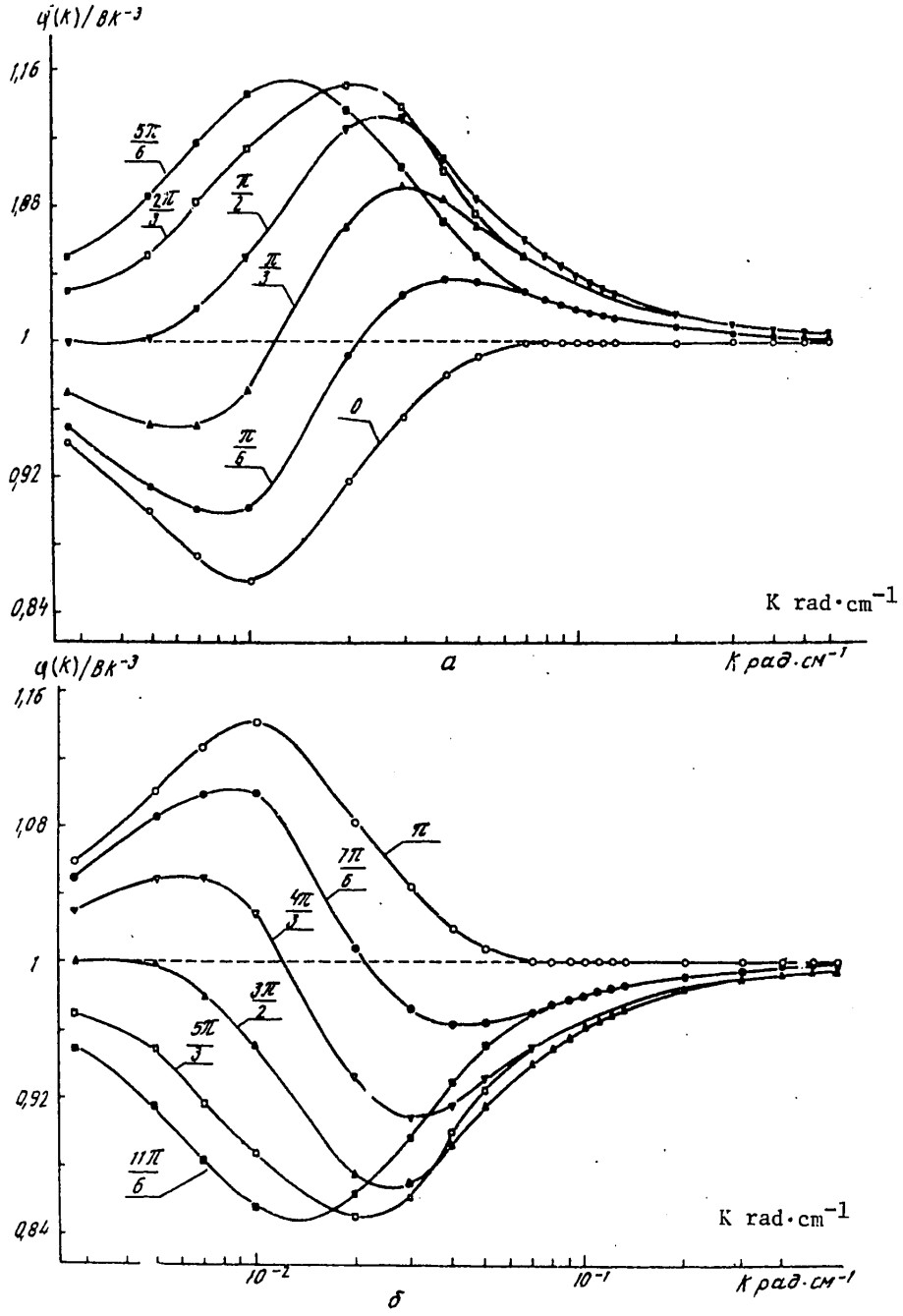

Fig. 2. Normalized spectrum of surface waves for different phases $k_1 x$ of internal wave.

For the short-wave spectral region with a high accuracy $\varphi(k) = \varphi_0(k)$. This result follows from an evaluation of the terms in equation (4). Since in the region of trapped waves $\omega_i/\alpha \ll 1$, this inequality is intensified with an increase in k and accordingly, with movement of the packet with a high accuracy there is satisfaction of the expression

$$\alpha(\varphi - \varphi^2/\varphi_0) \simeq 0,$$

that is, in each phase of the internal wave $\varphi(k) \simeq Bk^{-3}$. In the case of small wave numbers close to the wave number of the spectral peak the parameter $\omega_i/\alpha \gg 1$, that is, the long waves behave almost as free waves. The relative changes in spectral density are of the order of U_m/c_g [6].

In order to comprehend the physical side of the investigated phenomenon and explain the behavior of the φ spectrum in its energy-carrying part we will rewrite equation (4) in the following way:

$$\frac{d\varphi}{dt} = -\frac{1}{2}\varphi\frac{dU}{dx} + \alpha\varphi - \alpha\frac{\varphi^2}{\varphi_0}. \qquad (23)$$

The new term on the right-hand side is related to a different writing of the energy expression and represents the rate of change in wave packet energy associated with the work of radiation stresses during its interaction with an internal wave. In the internal wave phase from 0 to $5\pi/6$ (Fig. 2,a) $\partial U/\partial x < 0$, and accordingly, the internal wave simultaneously with the wind is a source of surface wave energy. The spectral level increases until the energy loss $\alpha \cdot \varphi^2/\varphi_0$ exceeds the source, after which the spectral level decreases. It is easy to determine the phase of the internal wave at which for the selected k value the spectrum of surface waves will be maximum (the energy sources are equal to the losses). This phase is determined from the equation

$$k_i x + \theta(k) = \pi(2n+1).$$

Figure 2,b illustrates the evolution of the normalized spectrum in the internal wave phase from π to $11/6\,\pi$. In this phase interval $\partial U/\partial x > 0$. Here the internal wave draws energy from the surface waves and the wind, as before, is a source. In this case the spectral density in the energy-carrying part of the spectrum almost everywhere drops off.

We note in conclusion that the relative changes in the wind wave spectrum under the influence of an internal wave can attain (Fig. 2) 16%. This circumstance can be decisive in the problem of sensing of internal ocean waves by remote methods.

BIBLIOGRAPHY

1. Phillips, O. M., "Interaction Between Internal and Surface Waves," IZV. AN SSSR: FAO (News of the USSR Academy of Sciences: Physics of the Atmosphere and Ocean), 9, No 2, pp 954-961, 1973.

2. Pelinovskiy, Ye. N., "Linear Theory of Forming and Variability of Wind Waves in a Weak Wind," IZV. AN SSSR: FAO, 14, No 11, pp 1167-1176, 1978.

3. Basovich, A. Ya., "Transformation of the Spectrum of Surface Waves Under the Influence of an Internal Wave," IZV. AN SSSR: FAO, 15, No 6, pp 655-661, 1979.

4. Voronovich, A. G., "Propagation of Internal and Surface Gravitational Waves in the Approximation of Geometrical Optics," IZV. AN SSSR: FAO, 12, No 8, pp 850-857, 1976.

5. Basovich, A. Ya. and Talanov, V. I., "Transformation of Short Surface Waves in Nonuniform Currents," IZV. AN SSSR: FAO, 13, No 7, pp 766-773, 1977.

6. Kuftarkov, Yu. M. and Kudryavtsev, V. N., "Determination of the Spectral Characteristics of Internal Waves in the Ocean by Remote Sounding Methods," IZV. AN SSSR: FAO, 1980 (in press).

7. Hughes, B. A., "The Effect of Internal Waves on Surface Wind Waves. 2. Theoretical Analysis," J. GEOPHYS. RES., Vol 83, No 1, pp 455-465, 1978.

8. Longuet-Higgins, M. S. and Stewart, R. W., "Changes in the Form of Short Gravity Waves on Tidal Currents," J. FLUID. MECH., Vol 8, No 4, pp 565-583, 1960.

5303
CSO: 1865/163

UDC 432.593

APPROXIMATE SOLUTIONS FOR INTERNAL WAVES IN A MEDIUM WITH AN ARBITRARY STABILITY DISTRIBUTION

Sevastopol' MORSKIYE GIDROFIZICHESKIYE ISSLEDOVANIYA in Russian No 1(88), Jan-Mar 80 (manuscript received 19 Oct 79) pp 56-64

[Article by V. V. Gorbatskiy]

[Text] Abstract: Asymptotic methods were used in investigating the properties of the dispersion relationships for internal waves propagating in a thermocline with an arbitrary distribution of the Väisälä-Brent frequency.

Nonstationary plane wave movement in a medium characterized by the stability parameter $\mathcal{E} = -\frac{1}{\rho}\frac{d\rho}{dz}$ (or the Väisälä-Brent frequency), in a linear approximation with use also of the Boussinesq approximation, is described by the equation [1]

$$N(z) = \sqrt{-\frac{g}{\rho}\frac{d\rho}{dz}}, \qquad \frac{\partial}{\partial t^2}\left(\frac{\partial^2 W}{\partial x^2} + \frac{\partial W^2}{\partial z^2}\right) + N^2(z)\frac{\partial^2 W}{\partial x^2} = 0 \tag{1}$$

for the vertical component of the velocity of vertical movement.

By the introduction of the dimensionless variables

$$\bar{x} = \frac{x}{L}, \quad \bar{z} = \frac{z}{L}, \quad \bar{t} = t\left(\frac{g}{H}\right)^{1/2},$$

where L, H are the horizontal and vertical linear scales respectively, equation (1) for plane internal waves $w(z)e^{-i(kx+\omega t)}$ is reduced to the form

$$\frac{d^2 W(z)}{dz^2} + \gamma^2\lambda^2\left[\frac{f(z)}{\gamma^2\sigma^2} - 1\right]W(z) = 0, \tag{2}$$

where

$$f(z) \equiv \mathcal{E}(z) = -\frac{1}{\rho}\frac{d\rho}{dz}, \quad \gamma \equiv \frac{H}{L}, \quad \lambda = kL, \quad \sigma \equiv \frac{\omega}{(g/H)^{1/2}}.$$

In combination with the approximate boundary condition at the free surface w = 0 with z = 0 and the boundary condition at the bottom w = 0 with z = -D equation (2) is a boundary-value problem for eigenvalues with the parameter λ^2, whose solution makes it possible to establish the dispersion relationships $\sigma = \sigma(k)$.

At the present time the dispersion relationships for internal waves in the ocean are investigated theoretically by two principal methods.

The method of schematization of a specific distribution of stability by uniform layers separated by infinitely thin density jumps has been developed to the greatest degree. In this case the finding of the dispersion relationships essentially involves a determination of the roots of a system of algebraic equations arising as a result of satisfaction of the boundary conditions at the interfaces of the layers [2-5].

The method of determining the dispersion relationships based on a schematization of the density distribution by layers with a constant value of the stability parameter

$$E = -\frac{1}{\rho}\frac{d\rho}{dz},$$

separated by density jumps, is more general but requires the carrying out of unwieldy computations.

Both methods in actuality consitute an approximation of the dispersion relationships for internal waves in a medium with a real density distribution. They can be called "a priori" because they provide for a preliminary schematization of density and subsequent formulation of corresponding precise dispersion relationships.

The generalization of such "a priori" approximations can be accomplished by constructing schematic profiles of the vertical distribution of the E parameter of a more complex form, but also leading to precise dispersion relationships.

As demonstrated in [6], such a class of profiles of the stability parameter E, described by a nonmonotonic function, includes: a parabolic vertical distribution; a distribution in the form of hyperbolic functions; a power-law distribution.

A fundamental shortcoming of the indicated methods for determining the dispersion relationships is the lack of any possibility for evaluating the error in the approximately determined dispersion relationships due to the arbitrary choice of the density distribution scheme.

An alternative method for determining the approximate dispersion relationships for internal waves in the ocean is their formulation by uniform asymptotic solutions of equation (2) with the arbitrary function f(z).

In such a method for formulating the dispersion relationships an important circumstance is the choice of the parameter from which the asymptotic solutions are sought.

Henceforth we will assume the parameter of the boundary-value problem (2) to be the parameter b. The parameters making it possible to change the form of the Brent-Väisälä frequency profile will be determined in the following way.

We will construct a universal stability profile characteristic for the layer of the ocean medium containing the thermocline using the function

$$f_1(x) = Ae^{-k_1 z^2} + Be^{-k_2 z^2}. \tag{3}$$

By examining the typical profile of the stability parameter in Fig. 1 it can be established that the function describing it must satisfy at least the conditions

$$f_1(z_0) = 0, \quad f_1''(z_1) = 0, \quad f_1'(z_2) = 0, \quad f_2(z_2) = N_{max}. \tag{4}$$

With these taken into account the function $f_1(z)$ acquires the form

$$f_1(z) = A\left[e^{-\varkappa\varphi(z^2 - z_0^2) - \varkappa z_0^2} - e^{-\varkappa z^2}\right], \tag{5}$$

where

$$A = \frac{N_{max}}{e^{-\varkappa\varphi(z_2^2 - z_0^2) - \varkappa z_0^2} - e^{-\varkappa z_2^2}} = \frac{N_{max}}{e^{-\varkappa z_2^2}\left[e^{\varkappa(1-\varphi)(z_2^2 - z_0^2)} - 1\right]}.$$

The following relationship exists between the parameters $\varkappa$ and φ

$$\varkappa(z_0 - z_2) = -\frac{\ln\varphi}{1-\varphi}, \tag{6}$$

and between the parameters z_0, z_1, z_2 and the φ parameter there is the dependence

$$\frac{\ln\varphi}{1-\varphi}\,g\left[\varphi^{2-(1+\beta)} - 1\right] = 1 - \varphi^{1-(1+\beta)}, \tag{7}$$

where

$$\beta \equiv \frac{z_0^2}{z_1^2}, \quad g \equiv \frac{z_1^2}{z_0^2 - z_2^2}.$$

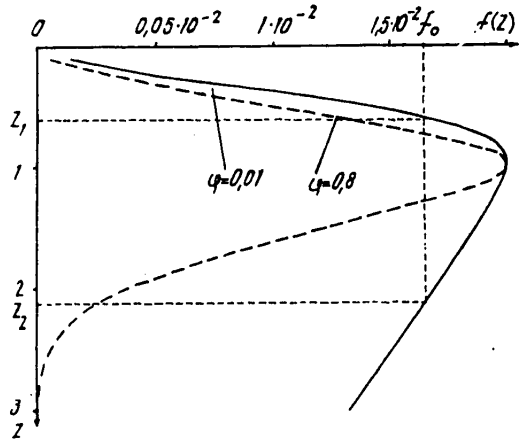

Fig. 1. Schematic distribution of stability for two extremal values of the parameter φ: 0.8 -- well-expressed thermocline; 0.01 -- blurred thermocline.

It follows from expression (6) that $0 < \varphi \leq 1$, since with passage through the point $\varphi = 1$ the function $f(\varphi, z)$ changes sign.

Thus, by varying the φ parameter, with stipulated z_0, z_1, z_2, N_{max} values it is possible to bring the profile (3) suitably closer to the real stability distribution.

Figure 2 shows the stability profiles corresponding to the values $\varphi = 0.8$ and 0.01 for the special cases $z_0 = 0$, $z_1 = 0$, $z_2 = -1$. Their comparison with the situation really existing in the ocean (Fig. 1) shows that the adopted approximations have all the characteristic features of a seasonal thermocline.

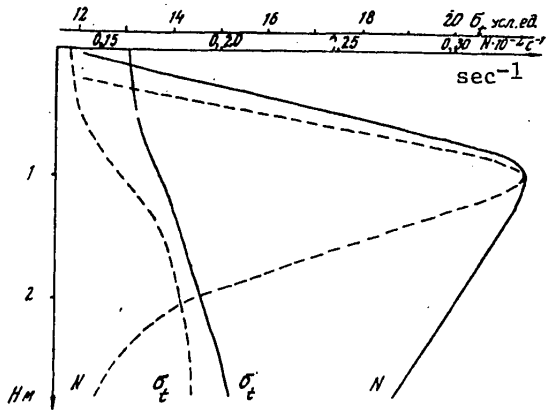

Fig. 2. Characteristic stability distributions in Black Sea and their schematization by a three-layer model (--- June, ___ October).

If the z values are assumed close to the horizon $z_2 = -1$ for a profile with the parameter $\varphi \approx 1$ or if the profile is approximated by the function $f(z, \varphi)$ with the value $\varphi \ll 1$, this function can be approximately represented in the form

$$\varphi \ll 1 \quad f(\varphi, z) \approx N_{max}^2 \left[1 - \varphi\left(z^2 - 1\right)\right] z^2; \tag{8}$$

$$\varphi \approx 1 \quad f(\varphi, z) \approx N_{max}^2 \left[1 - \varkappa\left(z^2 - 1\right)\right] z^2. \tag{9}$$

Such approximations are a corollary of asymptotic forms of the type

$$\begin{aligned} &\varkappa \to \infty && \varkappa\varphi \to 0 \\ &\varphi \to 0, && \varphi \to 0, \\ &\varkappa \to 1 && \varkappa\varphi \to 1 \\ &\varphi \to 1-0, && \varphi \to 1-0. \end{aligned} \tag{10}$$

Expressions (8) and (9) determine functions consisting of two branches symmetric relative to the horizontal plane z = 0; however, only the region $z < 0$ has physical sense, as was the case with the initial construction of the profile.

Further we will examine dispersion relationships in two approximations corresponding to the following values of the selected parameters δ and φ:

1) $\varphi \ll 1$, $\delta \approx N_{max}$, $\lambda \to \infty$. 2) $\varphi \approx 1$, $\delta \ll N_{max}$, $\lambda \to 0$.

This case corresponds to the propagation of short internal waves in a blurred thermocline.

Such a selection of values of the parameters corresponds to the propagation of long waves in a medium with a clearly defined thermocline.

1) As follows from Fig. 1, there are two points $z_{1,2}$, at which the following condition is satisfied

$$f(z) = \delta^2. \tag{11}$$

With the use of expression (8) the $z_{1,2}$ values are described by the expressions

$$z_{1,2} = -\left\{(\varkappa\varphi + 1)\left[\frac{1 \pm \sqrt{1 - \frac{4\varkappa\alpha^2}{(1+\varkappa)^2}}}{2\varkappa}\right]^{1/2}\right\}, \tag{12}$$

where

$$\alpha = \frac{\gamma\delta^2}{N^2_{max}}.$$

In accordance with the general theory of equations of type (2) the fundamental solutions have an oscillating form under the condition $f(z) - \delta^2 < 0$ and an exponential form under the condition $f(z) - \delta^2 > 0$. Thus, in the interval $z_2 < z < z_1$ the solution of equation (2) in the considered case is oscillating and attenuates exponentially outside the indicated interval. Due to the adopted approximation of short internal waves such attenuation is great and therefore the wave motion described by equation (2) under these conditions can be considered as falling in the layer (z_2, z_1). Using the known results in [7] of asymptotic representations of the dispersion relationships in the short-wave region

$$\lambda_n = \left(n + \tfrac{1}{2}\right) 2\pi \left(\int_{z_1}^{z_2} \left(\frac{f(z)}{\delta^2} - 1\right)^{1/2} dz\right)^{-1}, \tag{13}$$

in the considered case λ_n can be represented in the following way:

$$\lambda_n = \left(n + 1/2\right) 2\pi \left[\left(\frac{\varkappa - \varphi}{\alpha}\right)^{1/2} \int_{z_1}^{z_2} \left\{\left[1 - \left(z^2 - 1\right)\varkappa\right] \left|z^2 - \alpha^2\right\}^{1/2} dz\right]^{-1}, \tag{14}$$

where z_1 and z_2 are described by the expression (12).

With more rigorous limitations $\varkappa \to 1$, $\varkappa\varphi \to 0$ the integral form of the dispersion relationship can be reduced to the form

$$\lambda_n = \left(n + 1/2\right) \pi\alpha\varkappa^{-1/2} \left[\left(z_1 - 2\right)\sqrt{2}\left(1 - z_1\right)^{1/2} - \right. \tag{15}$$

$$-z_1^2 \cdot \ln\left(\frac{z - z_1 + \sqrt{z}(1 - z_1)^{1/2}}{z_1}\right)\Bigg]^{-1}, \tag{15}$$

where $$z_1 = \left(\frac{1 + \varphi - \alpha^2}{\varphi}\right)^{1/2}.$$

The limiting value of the error in the dispersion relationship (14), according to the results in [7], can be written in the form

$$\varepsilon \leq 1/4 \exp\left(-\frac{1}{\lambda}\int_{\infty}^{c} \frac{1}{[f(z)]^{3/4}} \frac{d^2}{dz^2}\left(f^{-1/4}(z)\,dz\right)\right) + \tag{16}$$

$$+ 1/4 \exp\left(-\frac{1}{\lambda}\int_{\infty}^{c} \frac{1}{[f(z)]^{3/4}} \frac{d^2}{dz^2}\left(f^{-1/4}(z)\right)dz\right) - 1/2,$$

where $c = i\infty$.

Using expression (8), after a series of transformations we establish the following form of the integrands in (16)

$$J = \frac{2\left[1 - \varphi z^2(1-\varphi) + \varphi^2(1 + 2z^4)\right]}{z^4\left[1 - \varphi(z^2 - 1)\right]^3}. \tag{17}$$

Expression (17) makes it possible to establish that with the selected λ value the magnitude of the error ε decreases with a decrease in φ and with $\varphi \to 0$ is $\delta = 0$. It is thereby shown that there is an analogy of the asymptotic approximations of the dispersion relationship for internal waves in the thermocline with $\lambda \to \infty$ and fixed values of the parameters of the E profile and with $\varphi \to 0$ and a fixed value of the λ parameter. Such an analogy can be used in a study of the characteristics of forced internal waves propagating in the thermocline for determining the regions of wave numbers in which the approximation of a real distribution of the E parameter by a scheme with a constant E value is applicable. In this case there is a considerable simplification of the analysis of the characteristics of the field of forced internal waves.

2) We will investigate the dispersion relationships in the approximation of long waves on the basis of the results indicated in [8]. Equation (2) can be represented in integral form

$$W(z) = \frac{1}{2}\lambda \int_{-\infty}^{0}\left(e^{-\kappa|y-\eta|} - e^{\kappa(2d - y - \eta)}\right) W(\eta)\, dF(\eta),$$

where

$$F(z) = \int f(z)\,dz, \quad \lambda = \left[\frac{\left(\rho(z_2) - \rho(z_1)\right)}{\rho(z_2) + \rho(z_1)}\right]\frac{g}{\kappa V_{BB}^2},$$

d is the depth of the maximum f(z) value.

As indicated in [8], there is an approximate relationship with $k \to 0$

$$\lambda_1 = \kappa L_0\left(1 + \kappa L\right),$$

where L_0 is the characteristic scale which has the evaluation $L_0 \to +d$ when $L \to 0$;

$$L = 2\int_0^\infty \frac{(\rho-\rho_+)(\rho_- - \rho)}{(\rho_- - \rho_+)^2}\, dy -$$

is the characteristic thickness of the thermocline.

Obviously, there is a relationship

$$L = z_2 - z_1 ,$$

where $z_{1,2}$ are established as roots of the equations

$$\rho_+ = -A\,\varkappa/2\left(z_+^2\left(z_+^2\left(z_+ - 1\right)-1\right)\right), \tag{18}$$

$$\rho_- = -A\,\varkappa/2\left(z_-^2\left(z_-^2\left(z_- - 1\right)-1\right)\right). \tag{19}$$

The ρ_+ and ρ_- values can be selected as limiting values for the interval of the main change in density in the entire thickness of the medium.

Using expressions (18), (19), we establish the asymptotic evaluation

$$L \to 0$$

and thereby

$$\varphi \to 1-0$$

$$\lambda_1 \to +kd$$

$$\varphi \to 1-0 .$$

If we then use the approximate expression

$$V_{gg}^2 = V_0^2\left[1 - kL + O\left(k^2 d^2\right)\right], \tag{20}$$

where

$$V_0^2 = \frac{\Delta\rho}{\rho}\, gh .$$

obtained in [9], we will have the asymptotic evaluation

$$V_{gg}^2 \to V_0^2$$

$$k \to 0 .$$

At the same time, expression (20) makes it possible to obtain the evaluation

$$V_{gg}^2 \to V_0^2\left(1 - kh\right)$$

$$\varphi \to 1-0 .$$

Thus, the approximation of the dispersion relationship with $\varphi \to 1-0$ and a stipulated k value corresponds to an approximation with $k \to 0$ and a stipulated φ value and with a greater accuracy the lesser the k value in the first case.

In conclusion we will examine the computed characteristics of the dispersion relationships obtained using formula (15). It follows from the graphs represented in Fig. 3 that internal waves propagating in a medium with a profile characterized by small values of the φ parameter, that is, in the case of a blurred thermocline, exceed the phase velocities in a medium with a sharply expressed thermocline (greater values of the parameter φ), at least for wave movements with frequencies close to the maximum value.

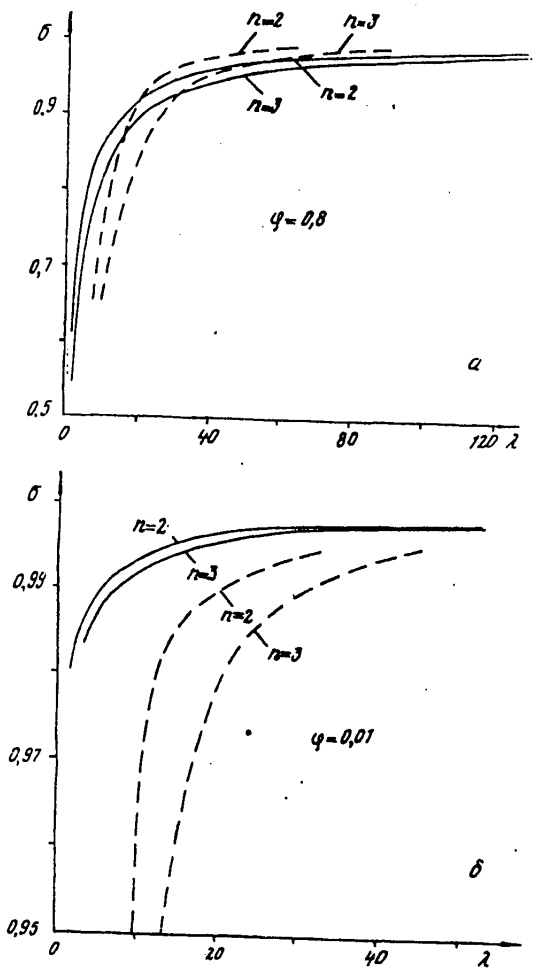

Fig. 3. Dispersion relationships in the case of a sharp (a) and a blurred (b) thermocline (- - - computations using a three-layer model; ___ using formula (15)).

Figure 3 gives a comparison of the asymptotic dispersion relationships with those obtained on the basis of a schematization of the distribution of the E parameter by a three-layer model. We note that for the density profile corresponding to a sharp thermocline the schematization leads to understated values of the phase velocities with small wave numbers and their exaggeration in the case of large wave numbers. The schematization of the blurred thermocline by a three-layer model causes an understatement of the phase velocities in the entire considered range of wave numbers and in an increasing degree in the region of small wave number values.

BIBLIOGRAPHY

1. Phillips, O. M., DINAMIKA VERKHNEGO SLOYA OKEANA (Dynamics of the Upper Layer of the Ocean), Moscow, "Mir," 1969, 267 pages.

2. Gorbatskiy, V. V. and Ivanov, G. N., "Propagation of Internal Waves in a Medium With Density Microjumps," TEORIYA DIFRAKTSII I RASPROSTRANENIYA VOLN (VII VSESOYUZNYY SIMPOZIUM PO DIFRAKTSII I RASPROSTRANENIYU VOLN) (Theory of Wave Diffraction and Propagation (VII All-Union Symposium on Wave Diffraction and Propagation)), Vol 2, Moscow, pp 298-300, 1977.

3. Sannikov, V. F. and Cherkesov, L. V., "Development of Propagating Internal Waves Generated by Moving Disturbances," MORSKIYE GIDROFIZICHESKIYE ISSLEDOVANIYA (Marine Hydrophysical Research), No 3, Sevastopol', pp 5-18, 1977.

4. Hyun, J. M., "Internal Wave Dispersion in Deep Oceans Calculated by Means of Two-Variable Expansion Techniques," J. OCEANOGR. SOC. JAP., 32, No 1, pp 11-20, 1976.

5. Friegel, M. and Hunkins, K., "Internal Wave Dispersion, Calculated Using the Thomas-Huskell Method," J. PHYS. OCEANOGR., 5, pp 541-548, 1975.

6. Headling, J., "Barriers Bounded by a Transient Point of Order Greater Than Unity," PHYSICA, Vol 77, Part 2, pp 263-278, 1974.

7. Oliver, F. W., "Error Analysis of Phase Integral Methods. 2. Application to Wave-Penetration Problems," J. RES. NAT. BUR. STANDARDS, Vol 69, No 4, pp 291-300, 1965.

8. Miles, I. W., "Internal Waves in a Sheeted Thermocline," J. FLUID MECH., 53, No 3, pp 557-573, 1972.

9. Benjamin, T. B., "Internal Waves of Permanent Form in Fluid of a Great Depth," J. FLUID MECH., 29, 3, pp 559-592, 1967.

5303
CSO: 1865/163

UDC 551.466.8:551.465:5(261.5)

INVESTIGATION OF INTERNAL WAVES AND MESOSCALE VARIABILITY OF CURRENTS IN THE EQUATORIAL ATLANTIC

Sevastopol' MORSKIYE GIDROFIZICHESKIYE ISSLEDOVANIYA in Russian No 1(88), Jan-Mar 80 (manuscript received 14 Nov 79) pp 180-187

[Article by V. V. Yefimov]

[Text]

Abstract: The article discusses some results of experimental investigations carried out on the 20th voyage of the scientific research ship "Akademik Vernadskiy." The data obtained in a mesoscale polygon were processed by a special method and the spatial-temporal spectra of internal waves were determined in the region of tidal components. Prolonged measurements of currents at three simultaneously operating automatic buoy stations revealed wave fluctuations of velocity with a period of about 20 days and a wave length of about 1000 km. The probable nature of these fluctuations is discussed.

During the period May-July 1979 the scientific research ship "Akademik Vernadskiy" carried out work under the program of the First Global Experiment (FGGE) in the equatorial region of the Atlantic Ocean. In addition to the carrying out of mandatory meteorological, aerological and hydrological studies, the specialists carried out an oceanographic program whose principal purpose was a study of the variability of the system of currents in the Equatorial Atlantic and internal waves. During the two observation periods of FGGE complex measurements were made in a special mesoscale polygon, systems of self-contained buoy stations were set out and measurements were also made on several meridional runs.

In general, the measurement data made it possible to study the variability of the system of currents in the Equatorial Atlantic in the region of synoptic scales and also the spatial-temporal characteristics of baroclinic fluctuations in the range of time scales from several hours to several days and spatial scales of about 10-100 km.

We will examine the measurement method and also some results of processing data and their preliminary interpretation.

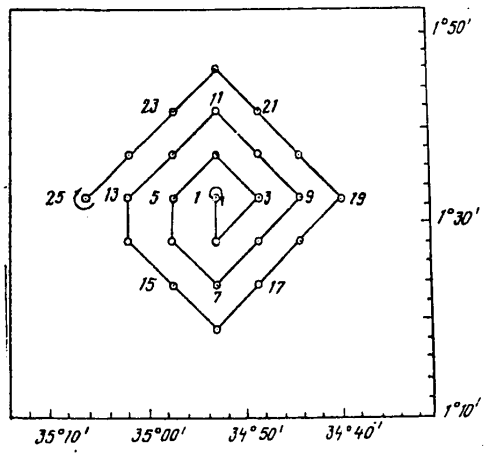

Fig. 1. Diagram of polygon.

1. A special polygon was planned and worked for a study of the energy characteristics of baroclinic fluctuations and computations of the spatial-temporal spectra of internal waves determining the distribution of the energy of waves by frequencies and wave numbers. It consisted of a network of hydrological stations arranged in accordance with the scheme shown in Fig. 1. Vertical sounding of temperature and salinity to a depth of 1500 m with an automated complex of instrumentation was carried out at each station. The measurement time at a station was less than 1 hour and the discreteness in occupying successive stations was about 2 hours. A single survey of the polygon (execution of soundings from stations 1 to 25 and back) required about 4 days. Such surveys were repeated three times with small gaps between them. The total time for polygon measurements was 19 days.

In the course of the work the initial scheme of the polygon, while its general features were retained, was naturally deformed. The positions of the individual stations and the time they were occupied differed from the initially planned scheme and some soundings were not made. However, this was no obstacle to computation of the spatial-temporal spectra $E(\vec{k},\omega)$; here $\vec{k}$ is the wave number vector; ω is the wave frequency.

In the computations use was made of a method in which the $E(\vec{k},\omega)$ spectrum is determined using data from measurements of the hydrophysical characteristics at different points in the ocean and at different moments in time [1]. Data on the temperature measured at standard horizons in the region of the upper thermocline were used. The mathematical expectation of the evaluation $\hat{E}(\vec{k},\omega)$ is related to the true spectral density $E(\vec{k},\omega)$ by the expression

$$\left\langle \hat{E}(\vec{k},\omega) \right\rangle = \int_{\vec{\lambda}} \int_{\nu} E(\vec{\lambda},\nu) W(\vec{k}-\vec{\lambda},\omega-\nu)\, d\vec{\lambda}\, d\nu,$$

where $W(\vec{k},\omega)$ is the spectral window of transmission in the region of wave numbers and frequencies, and was determined numerically for this polygon.

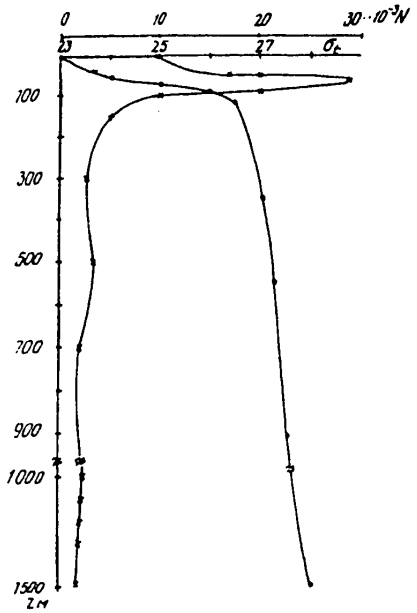

Fig. 2. Averaged vertical profiles σ_t and N(z) in upper layer of the Equatorial Atlantic.

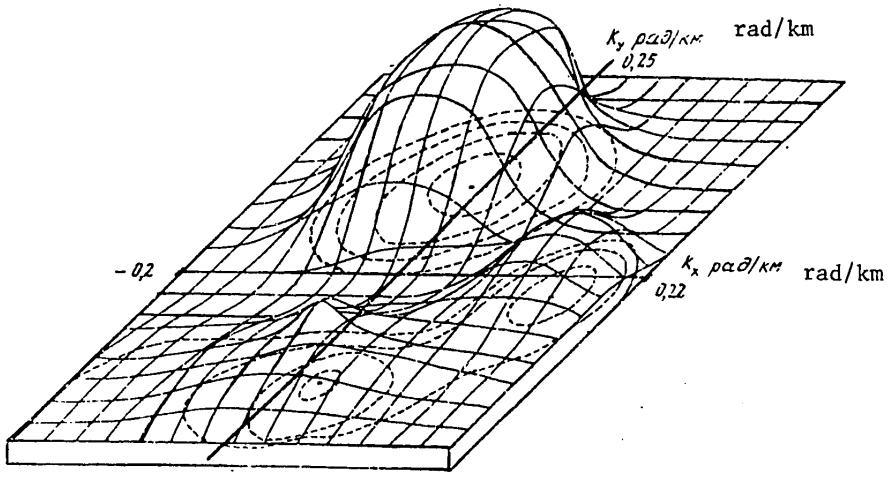

Fig. 3. Spatial-temporal spectrum of internal waves $E(\vec{k}, \omega)$ (in relative units) for ω = 0.52 cycle/day.

The spectral processing of measurement data makes it possible to formulate the following conclusions concerning the structure of the field of internal waves in the range of periods from several hours to 2-3 days.

First, the total dispersion of the temperature fluctuations in this range of periods in the upper thermocline was relatively small. Scaled to the rise of the thermocline it corresponded to a mean square displacement value 2.5 m. The thickness of the upper quasihomogeneous layer was about 50 m. Figure 2 shows the vertical profiles of conventional density and the Brent-Väisälä stability frequency N. Thus, the polygon can be assigned to regions relatively calm with respect to internal waves. This probably is attributable to the meteorological regime of the Equatorial Atlantic, for which moderate wind velocity values are characteristic and sharp weather fluctuations are absent.

Second, the principal contribution to the energy of internal waves is from semidiurnal tidal oscillations. Figure 3 shows the spatial-temporal spectrum of internal waves $E(\vec{k}, \omega)$ for a frequency $\omega = 0.52$ cycle/day corresponding to a semidiurnal tide, k_x is directed to the east, k_y is directed to the north. It can be seen that the energy of the fluctuations is distributed nonuniformly by wave numbers for this frequency. There is a main maximum falling at values of the wave numbers $k_x = -0.01$, $k_y = 0.22$ rad/day. This is close to the wave number of the first baroclinic mode, computed on the basis of a simple two-layer model of the ocean. The position of the main spectral maximum (Fig. 3) approximately corresponds to the direction to the eastern extremity of the South American continent so that it can be assumed that these internal tidal waves are generated on the shelf of this continent as a result of transformation of a barotropic semidiurnal tide.

2. At the present time the fundamental pattern of the field of currents in the equatorial zone of the Atlantic Ocean is sufficiently known [2]. However, there is a considerable variability of the equatorial currents at synoptic scales. The studies made on the expedition made it possible to investigate some parameters of this variability and its influence on the advective transport of heat in the equatorial region. For this purpose in the region 35°00'W, 01°30'N three autonomous buoy stations outfitted with DISK and BPV-2 automatic current and temperature recorders were set out in an equilateral triangle arrangement during the period 10 May-6 July. During the period 23 June-3 July observations were made of currents and temperature at the three buoy stations most distant from one another at the points 03°00'N, 35°00'W; 01°30'N, 33°30'W; 00°00'N, 35°00'W. In addition, measurements were made of currents and temperature on a meridional run across the equator along 35°00'W using DISK instruments. The placement of the instruments was accomplished from aboard a drifting ship; the duration of the measurements was about 13 hours. In order to exclude drift velocity from the instrument readings use was made of a satellite navigational system, which made it possible to determine the mean velocity during the time of observations with an error of about 1 cm/sec.

Figure 4 shows the temporal change of the mean diurnal vectors at one of the three autonomous buoy stations in the region 01°30'N, 35°W; close results were obtained for the other two autonomous buoy stations situated at a distance of 7.5 miles. In the upper 100-m layer there is a zonal current of an easterly direction subjected to fluctuations in a meridional direction with a period of about 20 days. In the layer of depths 100-150 m the direction of the zonal easterly current changes to southwesterly and at a depth of 300 m the velocities attain 60-80 cm/sec. At a depth of 700 m there was a current of an easterly direction with a velocity 10-15 cm/sec. The presence of a powerful flow of an easterly direction in the layer 25-30 m is probably associated with the rising of the Lomonosov Current toward the

surface, which was sometimes observed in the eastern part of the Equatorial Atlantic. We note that the lower boundary of this current, which is usually registered at a depth of 200-300 m, also rose above 150 m. The mechanism of such considerable vertical fluctuations of the Lomonosov Current in the western part of the Atlantic still remains unstudied.

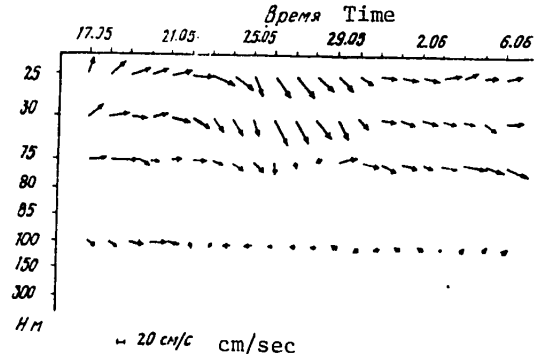

Fig. 4. Mean diurnal current vectors at several horizons in the region 01°30'N, 35°W.

Observations of currents from 23 June through 3 July gave results close to the known scheme of mean circulation for the Equatorial Atlantic. In the upper layer of the ocean to a depth of 50 m there was a westerly transfer and velocities at individual points attained 70-80 cm/sec. The Lomonosov Current is situated at depths from 50 to 200 m (velocities 60-70 cm/sec) and is traced to 01°30'N. To 04°00'N in the entire baroclinic layer there was a westerly transfer caused by the South Trades Current. Beginning at 04°30'N the easterly transfer by the Inter-Trades Countercurrent becomes significant.

The results of multiday measurements with the autonomous buoy station (Fig. 4) indicate that there is a strong variability of currents in the equatorial region. Such considerable changes in current velocities were registered earlier in different areas of the equatorial regions of the Atlantic, Pacific and Indian Oceans [3].

Usually such a variability of currents is associated with wave fluctuations of one nature or another. Usually two possible types of such fluctuations are considered. The first is the meandering of jet currents at the equator [4, 5]; the second is equatorial Rossby waves [6]. Both of these are characterized by meridional nonuniformity of the wave field, but they have different dispersion relationships. Stationary disturbances corresponding to a meandering countercurrent of an easterly direction are propagated to the east [4]. In contrast to this, the phase velocities of equatorial trapped waves are directed to the west.

We note that the registered fluctuations, as indicated in Fig. 4, are characterized by high velocities and a clearly expressed periodicity. This made it possible to use data from the three spatially separated autonomous buoy stations for evaluating the predominant periods, directions and phase velocities even with a relatively

short duration of the measurements made.

The table gives the computed amplitudes and initial phases of waves which have a period close to 21 days.

Table 1

Number of autonomous buoy station	Depth, m	Latitudinal component		Meridional component	
		cm/sec	rad	cm/sec	rad
2	25	4.45	0.841	26.69	-1.171
3	25	6.33	0.131	20.81	-1.310
1	85	28.61	-0.534	-2.29	0.204
2	85	24.44	-0.985	-1.33	-0.466
3	85	21.14	-1.116	-2.79	-0.724

On the basis of the phase relationships and the known distance between the autonomous buoy stations it was found that the phase velocities of the waves at the 25 and 85 m horizons have close values of about 50-53 cm/sec; their common direction is westerly. The lengths of the waves are 800-900 km and their projections onto the equator are 1000-1100 km.

The propagation velocity and wave length values determined in this way make it possible to carry out a comparison with known models. First of all we note that the direction of wave propagation in a general westerly direction does not coincide with the propagation of a stationary wave corresponding to a meandering current of an easterly direction. This is the main factor from which it can be assumed that the registered waves are associated with wave motion of the the type of equatorial trapped Rossby waves. For these from the dispersion relationship it is easy to obtain evaluations of the wave number ℓ for a stipulated frequency [6]. In our case for a period T = 21.6 days and a depth of 400 m for the first frequency mode of a barotropic trapped wave it is possible to obtain an evaluation of the wave length $\simeq$ 950 km. This corresponds sufficiently closely to the experimentally computed value (in projection onto the equator the experimental data give $\ell \simeq$1000 km). Thus, both the direction of propagation and the phase velocity of the registered waves are sufficiently close to the theoretical evaluation.

However, it is probably premature to draw any final conclusion concerning the nature of the wave fluctuations. This can be attributed to the appreciable differences of the wave motion from a barotropic type. Although the amplitudes of the wave velocity fluctuations of the predominant period change relatively little in the upper layer, their phases experience great changes. These changes can indicate a baroclinic character of the observed waves.

BIBLIOGRAPHY

1. Yefimov, V. V., "Method of Polygon Investigations of the Spatial-Temporal Spectra of Wave Processes in the Ocean," IZV. AN SSSR: FAO (News of the USSR Academy of Sciences: Physics of the Atmosphere and Ocean) (in press).

2. Khlystov, N. Z., STRUKTURA I DINAMIKA VOD TROPICHESKOY ATLANTIKI (Structure and Dynamics of Tropical Atlantic Waters), Kiev, "Nauk. Dumka," 1976, 164 pages.

3. Rybnikov, A. A., PREDVARITEL'NYY ANALIZ MATERIALOV IZMERENIY TECHENIY NA EKVATORE V PERIOD ATEP. TROPEKS-74. T. 2 (Preliminary Analysis of Materials From Measurements of Currents at the Equator During the GATE Period. TROPEKS-74. Vol 2), OKEAN (The Ocean), Leningrad, Gidrometeoizdat, 1976.

4. Nelepo, B. A., Korotayev, G. K. and Vasil'yev, A. S., "Variability of the Equatorial Subsurface Countercurrent in the Indian Ocean," OKEANOLOGIYA (Oceanology), Vol 19, No 1, pp 5-9, 1979.

5. Monin, A. S., "Meandering of Equatorial Currents," IZV. AN SSSR: MEKHANIKA ZHIDKOSTI I GAZA (News of the USSR Academy of Sciences: Mechanics of Fluid and Gas), No 3, pp 98-102, 1973.

6. Kraus, Ye., VZAIMODEYSTVIYE ATMOSFERY I OKEANA (Interaction Between the Atmosphere and Ocean), Leningrad, Gidrometeoizdat, 1976, 295 pages.

5303
CSO: 1865/163

TABLE OF CONTENTS FROM 'MARINE HYDROPHYSICAL RESEARCH' -- NO 1(88), 1980

Sevastopol' MORSKIYE GIDROFIZICHESKIYE ISSLEDOVANIYA in Russian No 1 (88), Jan-Mar 80 pp 212-213

[Text] CONTENTS

Theory of Currents and Waves

Methods for Computing Physical Fields in the Ocean and Analysis of the Results of Observations

5303
CSO: 1865/163

UDC 551.465

LARGE-SCALE AND SYNOPTIC VARIABILITY OF FIELDS IN THE OCEAN

Moscow KRUPNOMASSHTABNAYA I SINOPTICHESKAYA IZMENCHIVOST' POLEY V OKEANE in Russian 1981 (signed to press 12 Jan 81) pp 2, 168

[Annotation and table of contents from book "Large-Scale and Synoptic Variability of Fields in the Ocean", by Yuriy Aleksandrovich Ivanov, Institute of Oceanology imeni P. P. Shirshov, USSR Academy of Sciences, Izdatel'stvo "Nauka", 750 copies, 168 pages]

[Text] The book is devoted to investigation of physical mechanisms that determine the formation and variability of hydrophysical fields in the ocean.

The author constructs and realizes a forecast model of the structure of the ocean, a model of the upper layer, models of the response of the ocean to perturbations of the atmosphere, and models of hydrodynamic stability of the average state. Results of modeling are compared with data of measurements in the ocean.

The book is intended for oceanologists, meteorologists, hydrodynamicists, and undergraduate and graduate students of appropriate specialties.

Figures 85, tables 10, references 184.

Contents page

6610
CSO: 1865/184

UDC 551.461+551.351+577.472

COLLECTION OF ARTICLES ON MARINE GEOLOGY, GEOPHYSICS, PHYSICS AND BIOLOGY

Moscow KOMPLEKSNYYE ISSLEDOVANIYA PRIRODY OKEANA in Russian No 7, 1980 (signed to press 27 Nov 80) pp 284-287

[Annotation and table of contents from book "Multisided Investigations of the Oceanic Environment", edited by A. M. Gusev and Ye. G. Mayev, Izdatel'stvo Moskovskogo universiteta, 565 copies, 288 pages]

[Text] Annotation. This collection (the first collection appeared in 1970 and the sixth in 1978) contains material from the First Conference on Problems of the World Ocean held at Moscow University in January 1976. This seventh collection gives the principal results of geological, geomorphological and geophysical investigations of the sea floor, hydrological, geophysical and biological investigations of the seas and oceans.

Contents

5303
CSO: 1865/189

SEVERAL APPLICATIONS OF PARAMETRIC ANTENNAS IN OCEANOGRAPHIC RESEARCH

Moscow AKUSTICHESKIY ZHURNAL in Russian Vol 27, No 3, May-Jun 81 pp 471-473

[Article by V. I. Timoshenko, Taganrog Radio Engineering Institute imeni V. D. Kalmykov]

[Text] A new class of hydroacoustic apparatus with parametric radiating (and also receiving) antennas has appeared thanks to the possibilities for its utilization for investigating and understanding the oceans. Based on results obtained in laboratory and sea-trial conditions, we studied the possibilities for using parametric devices in oceanographic investigations for locating underwater and silt-covered objects, precision echo sounding and bottom profiling, recording of ocean-bottom ground sections, registration of sound-scattering layers, transmitting of highly-directional beams of white noise and compound signals, and checking and monitoring the parameters of traditional acoustical apparatus, etc. The results obtained correspond well with the general theory of parametric antennas [1,2], based on calculating the diffraction of interacting waves in a quasi-optical approximation.

The investigations were made with parametric radiators and multi-element antennas having a 2a diameter of the pump oscillator converters from 15 to 300mm with pumping frequencies f_0 from 20 to 12,000 kHz. The working difference frequencies F_- are in the range from 0.2 to 400 kHz. The sound pressure levels at the difference frequency reach 20,000 Pa (made at one meter). The axial and spatial distribution of the primary and secondary fields of emittance, amplitude-frequency, phase and dynamic characteristics, and also the directivity characteristics were experimentally investigated and theoretically calculated. The parametric antennas constructed have a number of substantial advantages over traditional antennas: a broad bandpass (the overlapping frequency has a factor of tens and even hundreds), a narrow directivity pattern (several degrees) with a low level of side lobes (up to -46 dB), a constancy of width of the directional characteristic in the band of working frequencies, small dimensions of the initial pump oscillator converters, etc. The aforementioned advantages compensate for the basic inadequacy of the pump oscillator converters, i.e., the relatively small conversion coefficient (not exceeding 10 percent). The measurements were made in the waters of the Black, Baltic, and Azov seas with natural reflecting objects (including schools of fish) and also in sapropelic lakes, hydroacoustic basins and on the field experimental base "Semga" in the Gulf of Taganrog. Studies of parametric antennas with one to six elements are also being carried out.

TABLE 1

Type of instrument	Working frequency F_{-}, kHz	Pulse level P_{-}				Width 2θ, 7, degrees	Pump oscillator converters				Signal shaping diagram	Channel power (electric) kW	Divider pulse, microsec.	Pulse rate, Hz
		PA	with Z, m	in F_{-}, kHz			State	f_0, kHz	2a, mm	Shape				
PGL-300	1–25	150	10	20		4,0±0,5	1	300	100	Flat topped	Beat	0,5	0,1–20,0	0,4–200,0
PGL-2	130	1500	10	130		3,5±0,5	28	420 and	75×75	Mosaic	2-channel	0,3×2	0,01–5,0	0,4–200,0
							(14+14)	536						
PGL-2A	50	200	10	50		3,5±0,5	28	406 and	75×75	Mosaic	2-channel	0,3×2	0,01–5,0	0,4–200,0
							(14+14)	456						
PGL-3	5–25	200	5	10		4,0±0,5	1	294	100	Reinforced	Beat	0,8	0,1–20,0	0,4–200,0

TABLE 2

Type of instrument	Range F_{-}, kHz	Pulse level P_{-}			Width 2θ, 7, degrees	Pump oscillator converters			Signal shaping diagram	Operating conditions
		PA	with Z, m	in F_{-}, kHz		f_0, mHz	2a, mm	Shape		
NAI-5	2–300	15	1	5	30,0±1,0	1,014 and 203	40 & 30	slightly convex, slightly concave	Beat	for basins
NAI-6	1–150	5	3	10	3,5±0,5	1,19	30	Flat topped	Beat	for basins
NAI-6M	10–100	5	3	10	3,5±0,5	1,43	30	Flat topped	Beat	for basins with large hydrostatic pressure
NAI-7	0,1–10	10	100	1	2,5±0,5	0,136	300	flat, multi-element	2-channel	for natural conditions
NAI-8	1–10	5	3	5	5,0±0,5	0,48	50	flat with segments	DSB	for basins with large hydrostatic pressure
NAI-8M	1–50	10	3	10	3,0±0,5	0,73	65	flat with segments	2-channel	for basins with large hydrostatic pressure
NAI-9	1–200	5	3	5	5,0±0,5 and 30,0±1,0	0,98 and 2,0	30 & 20	flat and slightly convex	Beat	for basins (digital display)

The basic characteristics of the parametric sonars (PGL), with which the measurements were made, are presented in Table 1. The devices were developed by workers at the electro-hydroacoustic and ultrasonic equipment department of the Taganrog Radio-Engineering Institute imeni V. D. Kalmykov (TRTI).

The low level of side lobes in the beam pattern of the parametric antenna practically eliminates the influence of bottom and surface reverberations which is illustrated by comparative echograms that were obtained using the PGL-2 and a traditional fish locator. This characteristic of the PGL is especially important in the study of near-surface and near-bottom objects and of phenomena in oceanographic research.

The narrow nonlobe directivity pattern made it possible to conduct precision echo-location of parts of the Black Sea bottom with the PGL. Echograms of a sloping area to a depth of 900m were obtained with an accurate registration of small irregularities.

The low frequency sound beam from parametric antennas penetrates gaseous silt and relatively dense layers of alluvial sand bottom which makes it possible to locate silt-covered objects (with the depth of gaseous sapropelic silt down to 16 m) with the PLG-2 and the PLG-3 and to outline the profile of the bottom layers down to a depth of several tens of meters.

The broad band of working frequencies of parametric radiators makes it possible essentially for the first time to record the frequency dependency of reflections, to conduct impedance measurements, and with correction of amplitude-frequency response to radiate white noise and signals of the compound spectrum (FM, Linear FM, and others) with a narrow nonlobe beam. Without electronic correction the magnitude of the sound pressure of the parametric antenna is $P \sim F_{-}^{n}$. The exponent n on linear areas of the amplitude-frequency response varies within insignificant levels from 1.5 to 1.8. But with broadband parametric radiators in the initial parts of the amplitude-frequency response, where the coefficient of frequency reduction f_0/F_{-} approaches 1,000, the exponent n smoothly increases from 0.4 to 1.5. In this area the change of the diffraction divergence of the wave of the difference frequency plays a noticeable role. Broad band parametric radiators have been put into a series of measuring instruments of the NAI type created in the Taganrog Radio-Engineering Institute. Basic characteristics of these devices are given in Table 2.

The parametric instruments created in the Taganrog Radio-Engineering Institute have been demonstrated several times at the USSR Exposition of National Economic Achievements (in 1974, 1977, 1978, 1980) and at international exhibitions in Hungary (1978), Czechoslovakia (1979), and France (OCEANEXPO-80 in 1980) and at others.

REFERENCES

1. Novikov, B.K., Rudenko, O.V., Soluyan, S.I., "The Parametric Emitter of Ultrasound," AKUSTICHESKIY ZHURNAL, 1975, Vol 21, No 4, pp 591-597.

2. Novikov, B.K., Rybacheck, M.S., Timoshenko, V.I., "Interaction of Diffracting Sound Beams and the Theory of Highly-Directional Radiators of Ultrasound," AKUSTICHESKIY ZHURNAL, 1977, Vol 23, No 4, pp 621-626.

CSO: 8144/1328-P

TERRESTRIAL GEOPHYSICS

UDC: 550.3

GRAVIMETRIC STUDIES OF THE OCEANIC EARTH'S CRUST

Moscow GRAVIMETRICHESKIYE ISSLEDOVANIYA ZEMNOY KORY OKEANOV in Russian 1980 (signed to press 22 Oct 80) pp 2, 240

[Annotation and table of contents from book "Gravimetric Studies of the Oceanic Earth's Crust", by Adonis Garif'yanovich Gaynanov, Izdatel'stvo Moskovskogo universiteta, 910 copies, 240 pages, illustrated]

[Text] This monograph summarizes the results of gravimetric measurements [photos?] taken by Soviet and foreign geophysicists; it discusses methods of taking readings, describes the equipment used and furnishes maps of gravity anomalies of the Pacific, Atlantic and Indian oceans averaged for one-degree squares. Density models of earth's crust and the lithosphere of central ocean ridges, troughs [craters] and intermediate regions between continents and oceans were designed on the basis of gravimetric and seismic data; oil-and gas-bearing sedimentary basins situated on the shelf and continental slope were identified.

Contents

10,657
CSO: 1865/188

PHYSICS OF ATMOSPHERE

UDC: 551.591

SPECTRAL AND INTEGRAL CLEARNESS OF ATMOSPHERE OVER LAKE BAYKAL

Novosibirsk SPEKTRAL'NAYA I INTEGRAL'NAYA PROZRACHNOST' ATMOSFERY NA OZERE BAYKAL in Russian 1980 (signed to press 16 Jan 80) pp 2, 73

[Annotation and table of contents from book "Spectral and Integral Clearness of Atmosphere Over Lake Baykal", by Galina Petrovna Panova, Izdatel'stvo "Nauka", 1000 copies, 72 pages]

[Text] This monograph deals with the patterns of changes in integral clearness of the atmosphere to solar radiation at different times of the year; it furnishes estimates of values of daily, annual and perennial integral clearness. A correlation was established between integral and spectral clearness of the atmosphere, and it was determined that there is aerosol attenuation in different parts of the spectrum of solar radiation for wavelengths ranging from 0.35 to 1 μm. Optical hygrometry was used to estimate the level of water vapor deep in the atmosphere over Lake Baykal.

This book will be of interest to specialists in the field of limnology, climatology, space meteorology, hydrobiology, hydro-optics, botany, as well as engineering and technical personnel concerned with problems of planning the location of industrial, transportation and resort facilities.

Illustrations 19; tables 7; bibliography lists 97 items.

Contents

10,657
CSO: 1865/187

- END -